Synthesis, Characterization of Zirconia and Molybdenum Doped on Silica: Study their Catalytic Activity for Oxidation of Sulphides

AMAL A. MUFTAH[1], RAMEJABI SAYYAD[2], SHOBHA WAGHMODE[3], SUPRIYA SHUKLA[2] and SHARDA GADALE[2,*]

[1]Faculty of Education, Bani Walid University, Bani Walid, Libya
[2]Department of Chemistry, Yashwantrao Mohite College of Arts Science and Commerce, Bharati Vidyapeeth (Deemed To Be University), Pune-411030, India
[3]Department of Chemistry, MES Abasaheb Garware College, (Affiliated to Savitribai Phule Pune University, Pune), Pune-411004, India

*Corresponding author: E-mail: dagade@rediffmail.com

To explore the structural, green methodology and thermal stability for synthesizing series of ternary mixed metal oxides were prepared by doping ZrO_2 and MoO_3 on SiO_2 (ZMS) by sol-gel method. Catalysts were examined by XRD, FT-IR, XPS, Raman spectroscopy, temperature programmed desorption (TPD) and TEM techniques. Both oxides showed the high stability with nanocrystalline nature and the catalytic activity of synthesized ZMS catalyst were tested for oxidation of sulfides to sulfoxides at room temperature. Gas chromatography was used to analyze the products. A high selectivity obtained by nicely controlled a variation of catalyst amount as well as amounts of oxidant applied. Recycling experiments explained that the synthesized ZMS catalysts can be recycled many times without major loss of their activity. The catalytic system provided a number of advantages including clean, use of green solvent and easy handling strategy for the synthesis of sulfoxides at mild conditions.

Keywords: Ternary mixed oxide, Catalytic activity, Sol gel method, Zirconia, Molybdenum oxide, Oxidation, Sulfides, Sulfoxides.

INTRODUCTION

Heterogeneous catalysis makes extensive use of mixed metal compounds, either as catalysts or support materials [1]. Mixed metal oxides may be applied in large scale in redox and acid-based catalytic reactions, which show electron transfer and surface polarization properties [2]. Supported catalysts are well known for catalyzing diverse reactions so leading many researchers to focused their research on the preparation of these catalysts. Introduction of ZrO_2 to other oxide catalyst may generate a new active site, as the zirconia is only transition metal shows different properties like oxidizing, reducing along with acidic and basic properties. The ion-exchanged redox activities of ZrO_2 was used in many catalytic reactions as support and promoter [3-6]. Dumont *et al.* [7] prepared ceria-zirconia-alumina catalyst using sol-gel process and reported that addition of ZrO_2 to ceria-alumina increased their thermal stability. Furthermore, Noronha *et al.* [8] prepared Ni catalyst supported on ZrO_2 and the effect of synthesized catalyst was studied for steam reforming of toluene and methane.

Zirconia oxide offers different types of chemical reaction such as condensation, oxidation, nitration, esterification and isomerization. Among these transform reactions, Lee *et al.* [9] synthesized ZrO_2 catalyst by precipitation process and tested their activity in the decomposition reaction, the activity of the prepared catalyst becomes function of calcination temperature and showed a volcano curve with a maxima at 900 ºC.

Sulphated zirconia became popular among all promoted ZrO_2 catalysts after Arata & Hino [10] reported treatment of zirconia with sulphuric acid, which showed extremely strong acidity for isomerization of *n*-butane to isobutene. After period of time, sulphated zirconia has been synthesized by several researchers and used for different reactions [11-14]. However, major disadvantage for sulphated zirconia SO_4/ZrO_2 is its fast deactivation at higher temperature which cause in the formation of SO_x and H_2S, also when the reaction medium contains H_2O, it forms sulphuric acid.

From literature, it is observed that high active catalysts can be prepared by the introduction of a second or third metal oxide to the system [15]. Few studies are focused on the preparation

of ZrO_2 as support on other metal oxides as most of researchers worked on synthesis of MoO_3 on different oxides such as WO_2/ZrO_2, CeO_2-ZrO_2, TiO_2-ZrO_2, but $ZrO_2/MoO_3/SiO_2$ as a ternary composition not studied. The development of environmental friendly and switchable catalytic systems for converting a single raw material into distinct high-value products is both an attractive concept and a challenging synthetic contest. Although there are numerous methods for producing sulfones and sulfoxides, few examples of selective synthesis of sulfones and sulfoxides *via* solvent and catalyst dependent oxidation of sulphides are reported [16,17]. Liu *et al.* [18] reported the first example of efficient and selective oxidation of sulfides to sulfones and sulfoxides using molecular oxygen under clean conditions. He *et al.* [19] pioneered a catalyst free protocol for the selective oxidation of sulphides with inorganic oxidant oxone in ethanol and water. Jiang *et al.* [20] recently developed a solvent-dependent selective synthesis of sulfones and sulfoxides *via* visible light-induced $UO_2(OAc) \cdot 2H_2O$-catalyzed oxidation of sulphides with phosphoric acid and water as additives in pure acetonitrile and an acetonitrile/*o*-xylene solvent mixture, respectively.

Therefore, the present work focused on the characterization and catalytic activity of prepared $ZrO_2/MoO_3/SiO_2$ (ZSM) catalysis synthesized by sol-gel method. These catalysts can be used for important reactions such as oxidation, nitration, alkylation and so on. In current study, the oxidation of sulphides was carried out at mild conditions, over these catalysts and showed higher catalytic activity as well as selectivity of products. The main purpose of present work was to study, understand acidity and surface morphology of ternary mixed oxide catalysts.

EXPERIMENTAL

Preparation of catalyst: The sol-gel process was used for preparation of ZrO_2 supported on MoO_3/SiO_2 with various zirconium loading (1, 5, 10, 15 and 20%). Zirconyl nitrate hydrate, ammonium heptamolybdate tetrahydrate and tetraethyl orthosilicate were used as zirconium, molybdenum and silica source respectively. For a typical procedure, 1% $ZrO_2/MoO_3/SiO_2$ (1ZMS) was synthesized by adding tetraethyl orthosilicate (40 g) in isopropyl alcohol (40 mL), mixed slowly with constant stirring, dissolving 24.6g of ammonium heptamolybdate tetrahydrate in minimum amount of water and heated at 80 ℃ for 30 min in sonicator. Then added slowly to isopropyl alcohol (IPA) solution with continuous stirring, dissolved (1.87 g) zirconyl nitrate hydrate in distilled water then slowly added to above solution, greenish gel was formed, dried and finally calcined at 500, 600 and 700 ℃ for 7 h. Similarly, catalyst with 5%, 10%, 15% and 20% ZMS were prepared with different amount of zirconyl nitrate hydrate.

Characterization: The crystallite size of the samples was determined by X-ray power diffraction (XRD) using Rigaku Ultima IV diffraction using Cu$K\alpha$ radiation and a Ni filter. The FT-IR spectra were recorded on Thermo Nicolet iS5 IR instrument at ambient conditions using KBr pellets with a resolution of 4 cm^{-1} in the range of 4000-400 cm^{-1}. The X-ray photoelectron spectroscopy (XPS) studies were carried out on a VSW scientific instrument using incident source with an energy of 1253 eV and a resolution of 0.9 eV vacuum of 10-8 torr was maintained

in the sample analyzer chamber. The temperature-programmed desorption (TPD) was used for the determination of degree of acidity of the samples using NH_3 as molecule.

RESULTS AND DISCUSSION

XRD studies: The XRD patterns of pure ZrO_2 and 5, 10, 15 and 20wt.% $ZrO_2/MoO_3/SiO_2$ are shown in Fig. 1. The diffraction angles of the synthesized samples were consistent with the standard XRD patterns. The prepared ZMS mixed oxide catalysts showed the characteristic peaks at 23.4º, 25.8º, 27.4º, 33.7º and 49.6º correspond to α-MoO_3 on SiO_2 support. The peaks at 30.22º, 35.00º, 50.31º and 60.12º of tetragonal zirconia present in the ZMS mixed oxide samples, while silica support is in amorphous nature but it helps the stabilization of tetragonal phase of zirconia. The obtained XRD peaks confirmed the formation of t-ZrO_2 over the surface of MoO_3/SiO_2 support. The average crystallite size was reduced from 16.5 nm to 7.0 nm.
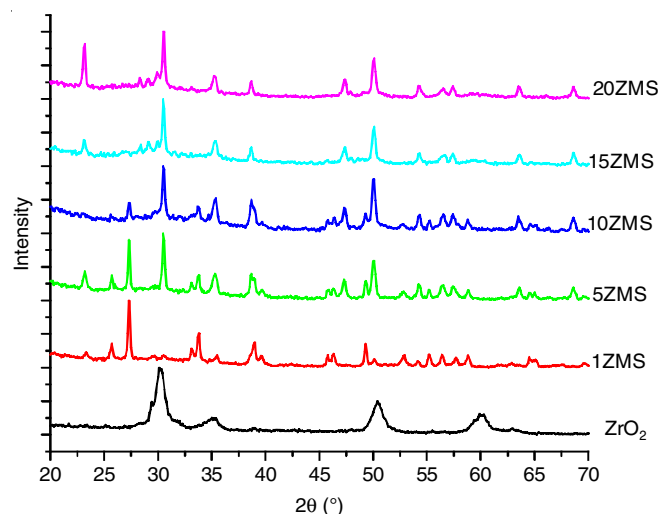

Fig. 1. XRD pattern of ZMS catalysts calcined at 500 ℃

From the above data, it was clearly confirmed the formation of t-ZrO_2 and α-MoO_3 phases in the prepared ZMS samples which were crystalline in nature. Furthermore, as the loading of zirconia over MoO_3/SiO_2 increased, there was hindrance of support, and thus support helps to reduce the crystallite size from sample 1ZMS to sample 20 ZMS. The effect of temperature was studied on the prepared catalysts to identify the stability of phases. Fig. 2 showed the XRD spectra of ZrO_2 calcined at 500, 600 and 700 ℃ and the crystallite phase was changes from tetragonal to monoclinic phase and showed the mixture of both phases.

The increased in calcination temperature *i.e.* 500, 600, 700 ℃ of the prepared catalysis showed its effect on phases as well as the size. As the prepared zirconia was present only in tetragonal phase in the samples calcined at 500 ℃, while after calcination up to 700 ℃, a mixture of tetragonal phase and monoclinic phase were observed. Hence, the phases changes to monoclinic at higher calcination temperature. Therefore, it is evident that the thermal stability of zirconia oxide strongly depends on the calcination temperature.
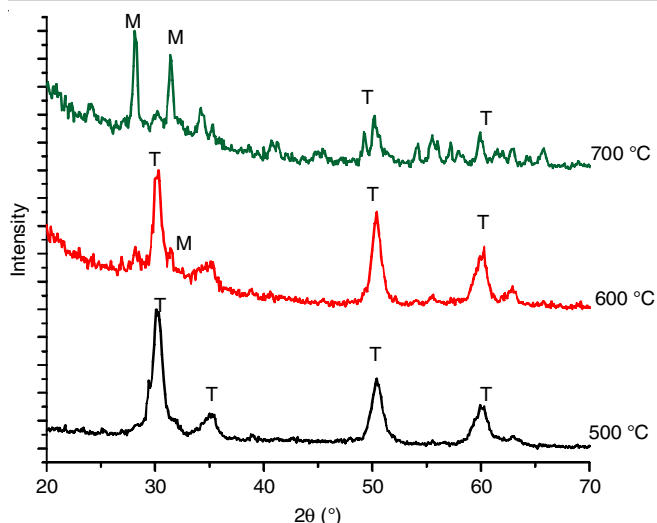
Fig. 2.   XRD pattern of ZrO$_2$ calcined at different temperature (M = monoclinic, T = tetragonal)

The effect of calcination temperature on crystallite size of synthesized catalysts are shown in Table-1. The size was calculated by Debye-Scherrer's equation. As calcination temperature increased the crystallite size also increased, which is attributed to the mixed phases of zirconia.

TABLE 1
EFFECT OF CALCINATION TEMPERATURE ON
CRYSTALLITE SIZE OF SYNTHESIZED SAMPLES

Sample	Calcination temperature (°C)	Crystallite size (nm)[a]
Pure ZrO$_2$	500	16.50
	600	16.99
	700	17.30
1ZMS	500	7.20
	600	7.30
	700	7.42
5ZMS	500	7.63
	600	7.39
	700	7.13
10ZMS	500	7.19
	600	7.40
	700	7.50
15ZMS	500	7.18
	600	7.57
	700	7.88
20ZMS	500	7.00
	600	7.20
	700	7.70

FTIR studies: The FT-IR spectrum of different loading of ZMS catalysts calcined at 500 °C are shown in Fig. 3. A peak at 740 cm^{-1} was assigned to the Zr-O-Zr asymmetric, while the band at 1380 cm^{-1} was assigned to Zr-O stretching modes. Also, the spectra showed a peak at 1000 cm^{-1} corresponds to the Mo=O and the peaks at 608 cm^{-1} due to O-Si-O bending mode. The peak at 1097 cm^{-1} was assigned to Si-O-Si stretch that conformed the formation of SiO$_2$ phase [21].

These spectra showed additional peak for the Si-O-Si stretching, while all other stretching were same. The results clearly showed peaks corresponding to Zr-O at 740, 1100 and
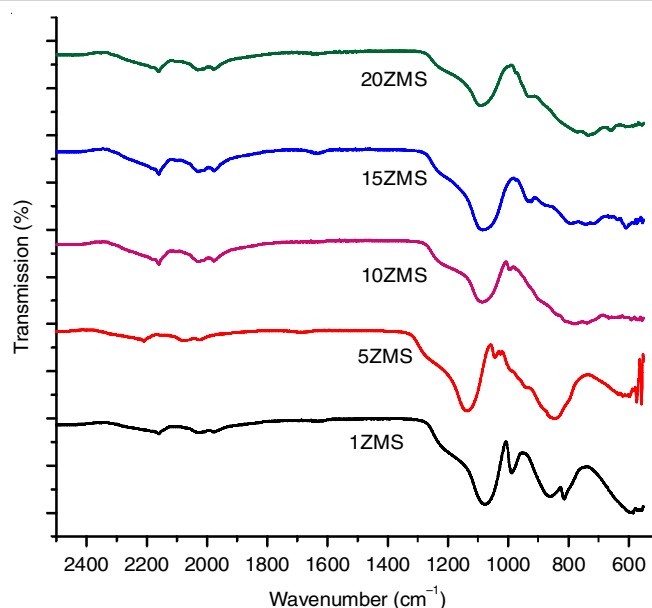

Fig. 3. FT-IR spectra of various % ZMS calcined at 500 °C

2170 cm^{-1} for all samples, even after heating at high temperatures, indicating the more crystalline nature. The molybdenum peak at 100 cm^{-1} was observed in the sample calcined at 500 °C.

Raman spectra: Raman spectra of pure ZrO$_2$ and various ZMS catalysts calcined at 500 °C are shown in Fig. 4. It is seen that pure zirconia sample showed diffe-rent peaks at 164, 270, 310, 466, 624 cm^{-1} which assigned to tetragonal phase of ZrO$_2$ [22], while the Raman spectra of ZMS mixed oxides revealed only the tetragonal phase of Zr, which is due to the presence of silica, which completely stabilized the t-ZrO$_2$ phase [23]. The observed Raman spectral lines for MoO$_3$ in ZMS samples (Fig. 4b) at 161, 285, 293, 339, 381, 666, 819 and 996 cm^{-1}, which correspond to α-MoO$_3$. As the amount of Zr increased in 15 ZMS and 20ZMS samples, the α-MoO$_3$ has shifted to 760 cm^{-1}, so all other lines were also shifted and thereby confirmed the addition of zirconia to the mixed oxide. The three low Zr loading samples show the same Raman lines at 660 and 248 cm^{-1} which are assigned to the silicomolybdic species [24].

Temperature programmed desorption (TPD) studies: The TPD spectra of ZrO$_2$ and prepared samples calcined at 500 °C are shown in Fig. 5. There are two distinct peak regions *viz.* one at low temperatures (T < 400 °C), indicating the presence of weak acid sites, and another at high temperatures (T > 400 °C), indicating the presence of strong acid sites. The results showed strong desorption peak observed at around 692 °C, it is generally reported that the surface acidity of zirconia is due to Zr^{2+} and OH$^-$ species. Incorporation of *d*-block metal ions modifies in more coordinated unsaturated cations and then generate more acidity.

The first sample 1% ZMS showed two small peaks one at high temperature and other at low temperature region (636.2, 234.2 mmol/g), which corresponds to the strong and weak adsorption sites, the total acidity in this sample was 0.057 mmol/g, which was the lowest acidity in ZMS series that might be due to presence of few weaker acid sites. Table-2 showed
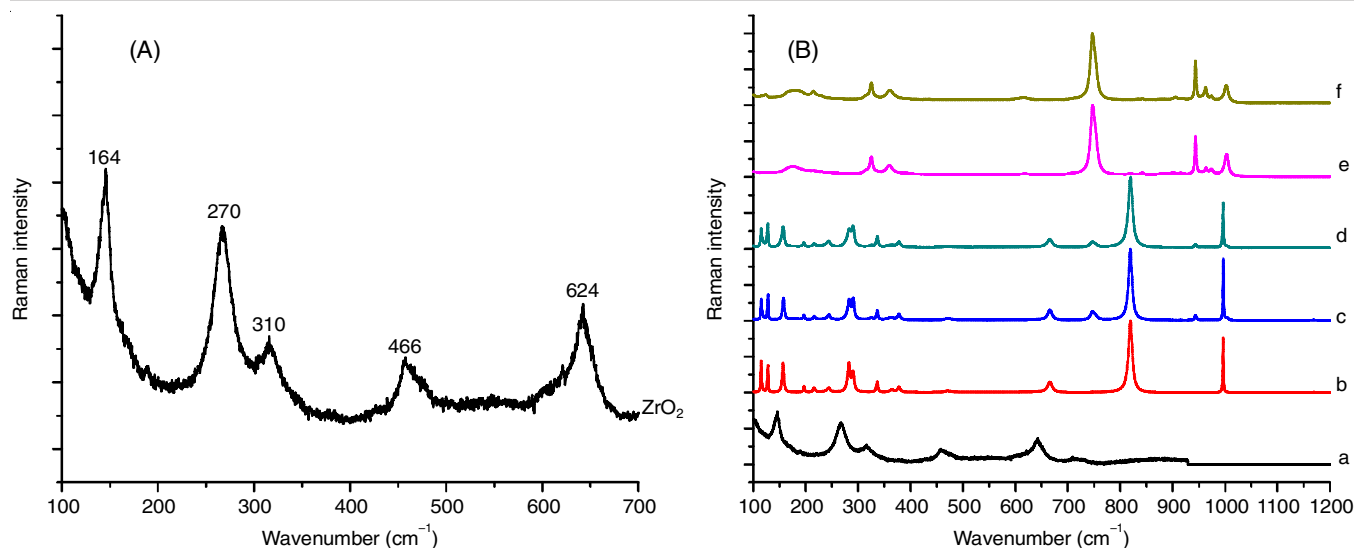
Fig. 4. Raman spectra of (A) pure ZrO_2 catalyst and (B) (a) ZR, (b) 1ZMS, (c) 5ZMS, (d) 10ZMS, (e) 15ZMS and (f) 20ZMS mixed oxide catalyst
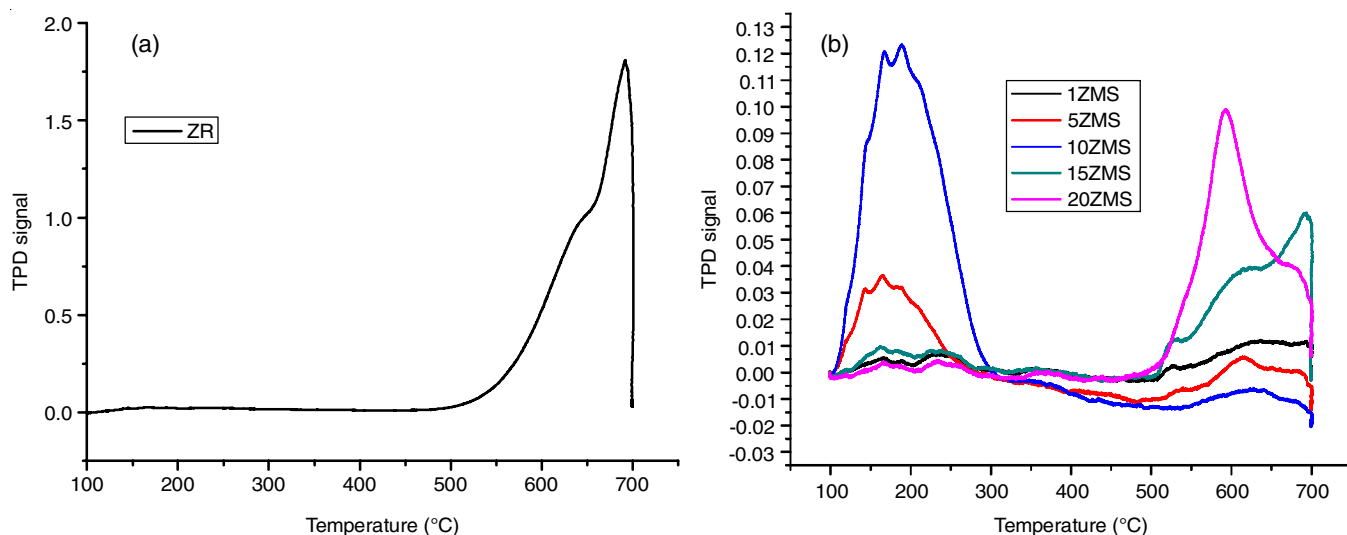

Fig. 5. TPD spectra of (a) ZrO_2 catalyst calcined at 500 °C and (b) different loading of ZMS catalysts

TABLE-2
ACIDITY MEASUREMENT OF THE PREPARED CATALYSTS

Sample	Peak at low temp.	Peak at high temp.	Acidity (mmol/g)
1 wt.% $ZrO_2/MoO_3/SiO_2$	234.3	636.2	0.057
5 wt.% $ZrO_2/MoO_3/SiO_2$	164.8	618.0	0.078
10 wt.% $ZrO_2/MoO_3/SiO_2$	192.3	649.7	0.181
15 wt.% $ZrO_2/MoO_3/SiO_2$	162.6	691.5	0.140
20 wt.% $ZrO_2/MoO_3/SiO_2$	–	600.0	0.130

that the total acidity increased with increasing of zirconia loading up to 10ZMS then decreased with further loading. The catalyst with 10ZMS loading showed the highest acidity in the series (0.181 mmol/g), however further loading above 10% show slightly decrease in the acidity due to the agglomeration of zirconia at higher loading. Thus, sample 10ZMS has the highest acidity as it has number of strong as well as weak acid sites are present in more amount. It is concluded that the total acidity of catalyst was increased due to both type of acidic sites, pres-

ence of Zr^{2+} and Mo^{6+} and hydroxyl groups attached to the support.

EDX studies: The data of EDX analysis showed presence of Zr, Mo, Si and O elements in the prepared samples and confirmed the composition of catalysts (Fig. 6). Therefore, the EDX confirmed the formation of $ZrO_2/MoO_3/SiO_2$ catalysts.

FESEM studies: The particle size and morphological feature of the prepared ZMS catalysts calcined at 500 °C can be obtained from field emission scanning electron microscope (FESEM) analysis. The results showed that the ZMS catalyst were agglomerated and aggregated each other on the surface, which form the rough surface morphology. Additionally, the sample was found to have a small particle size and numerous pores, both of which contribute significantly to the reported elevated catalytic activity.

The FESEM micrographic images of all the prepared samples are shown in Fig. 7. It was observed that the particles were agglomerated and almost spherical in shape with average
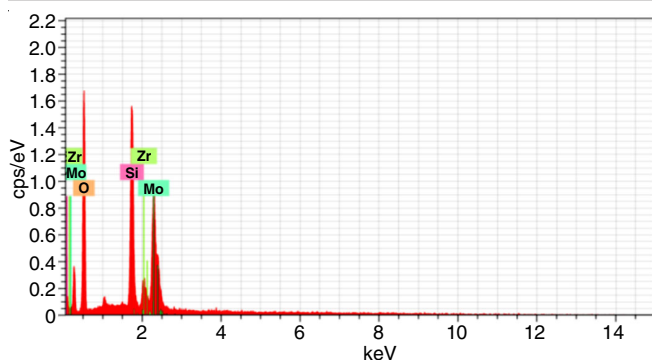
Fig. 6. EDX analysis of 10 wt. % ZMS catalyst

size range approximately between 9-39 nm. As the amount of zirconia increased, change in crystallite shape was prominently observed. The preparation method highly influences the particle size of the catalysts. Therefore, the nanoparticle sizes of all prepared catalysts were determined by combining the results of crystallite size obtained from XRD data and those obtained from FESEM.

TEM studies: The TEM images of zirconia and zirconia supported on MoO_3/SiO_2 at different loading are presented in Figs. 8 and 9, which confirmed the formation of the spherical morphology. The average particle size obtained from the TEM analysis was found to be in the range 6-20 nm, which is in good agreement with results obtained by XRD analysis. The small pores evenly distributed in the particle show the porous nature of the sample and the pores appear brighter than the surrounding ones because they absorbed less electrons [25]. Furthermore, the results highlight the fact that the prepared zirconia mixed oxide catalysts were slightly agglomerated and the particles are relatively uniform in size and shape.
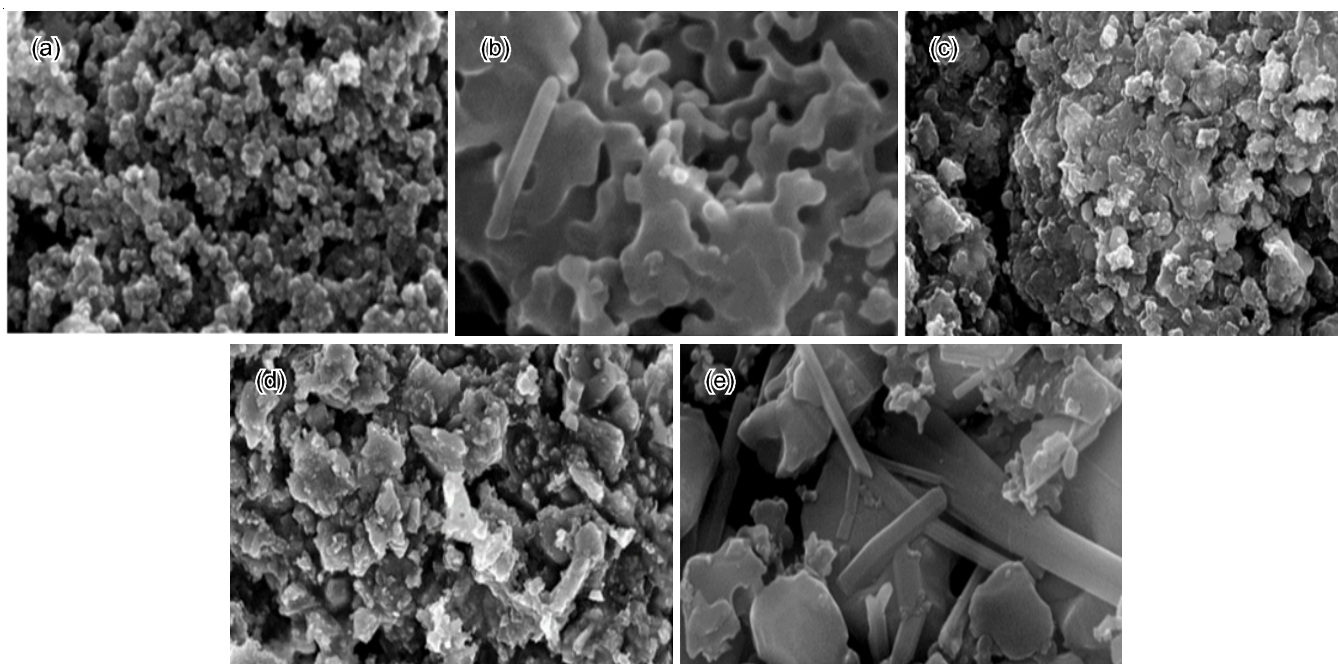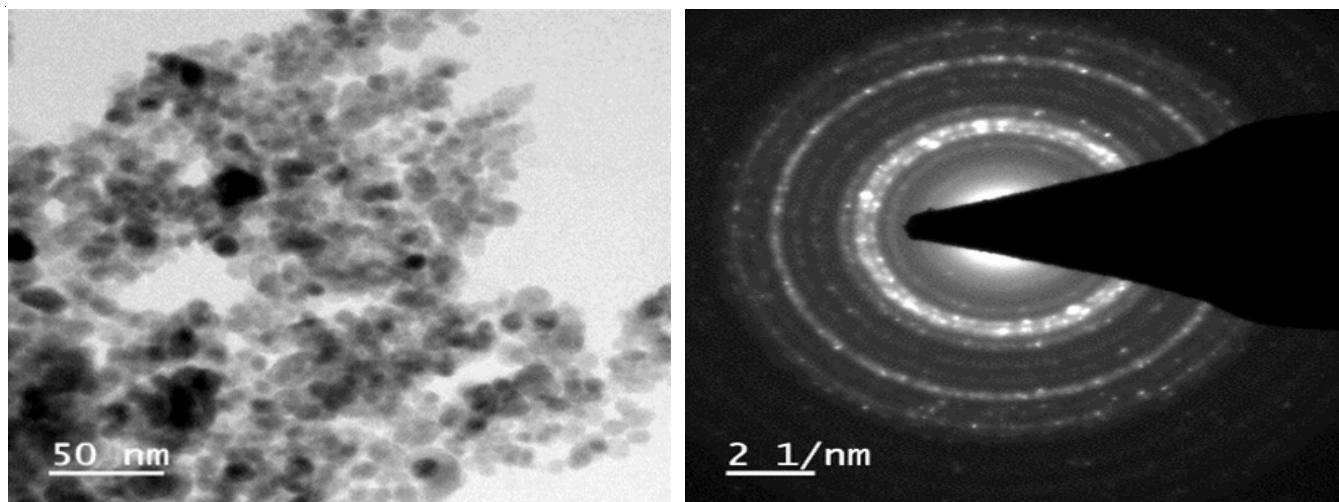

Fig. 7. FESEM images of a-e of 1-20 wt.% ZMS catalysts respectively

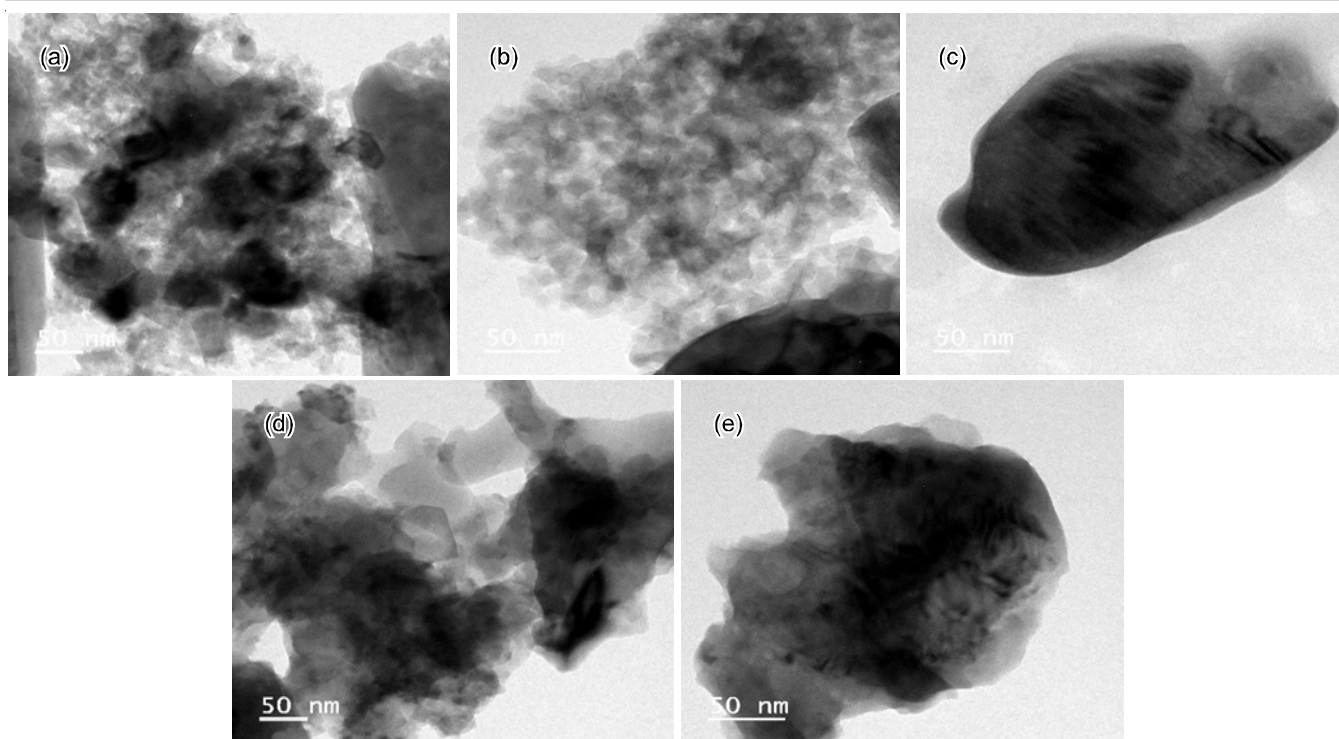Fig. 8. TEM micrograph of ZrO_2 catalyst at different magnification and focused on different areas

Fig. 9. (a-e) TEM micrograph 1-20 ZMS catalyst respectively

The TEM micrograph of 1ZMS catalyst showed the size of particles is still spherical as ZrO_2 added to MoO_3/SiO_2 (Fig. 9a). While in other samples (5ZMS, 10ZMS, 15ZMS and 20ZMS) exhibit the spherical sized particles with agglomeration, which may due to the addition of more amount of ZrO_2 on MoO_3/SiO_2.

XPS studies: The oxidation state of the elements present in prepared catalysts were investigated by X-ray photoelectron spectroscopy (XPS) technique. The binding energy values of Zr $3d_{3/2}$, Zr $3d_{5/2}$, Mo $3d_{3/2}$, Mo $3d_{5/2}$, Si $2p$ and O $1s$ are present in Table-3. The XPS peaks of Zr $3d$, Mo $3d$, Si $2p$ and O $1s$ were distinctly visible and confirmed the presence of these elements. For a better comparison, the XPS peaks of ZrO_2 in ZMS catalyst are presented together, also comparison has done with Mo, Si and O in these Figs. 10-14. The results clearly show that the XPS bands depend on zirconia coverage in MoO_3 oxide and MoO_3/SiO_2 mixed oxide conveyor.

Zr3d: The core level spectra of Zr $3d$ in ZMS samples are depicted in Fig. 10, which showed the XPS spectra of representative samples (5ZMS, 10ZMS and 20ZMS). The XPS peaks are distinctly visible and confirmed presence of Zr ($3d_{3/2}$, $3d_{5/2}$), Mo ($3d_{3/2}$, $3d_{5/2}$), Si ($2p$) elements. Here Zr $3d_{3/2}$ and Zr $3d_{5/2}$ observed their binding energies at 182.1 eV and 184.4 eV, respectively not much change with various ZrO_2 loadings, which provides the evidence of presence of a single type of zirconium oxide with an oxidation state of +4.
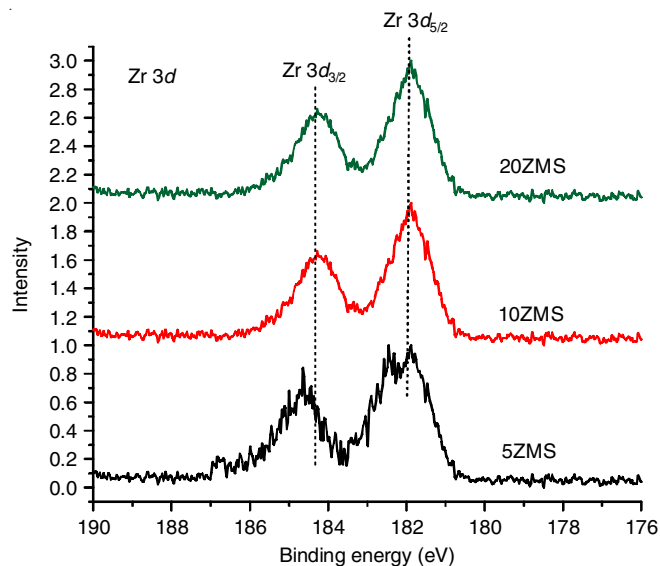
Fig. 10. Zr3d XPS spectra of the different composition of ZMS samples

Mo 3d: The energy line of Mo $3d$ spectra showed two peaks ($3d5_{5/2}$, $3d_{3/2}$) which can be related to the binding energy of spin orbit splitting of Mo(VI). All the samples showed the binding energy of Mo $3d_{3/2}$ and $3d_{5/2}$ level at around 232.29 ± 0.1 and 235.4 ± 0.1 eV, respectively as shown in Fig. 11, which correspond to the oxidation state of Mo(VI) [26].

TABLE-3
BINDING ENERGIES (eV) FOR $ZrO_2/MoO_3/SiO_2$ CATALYST

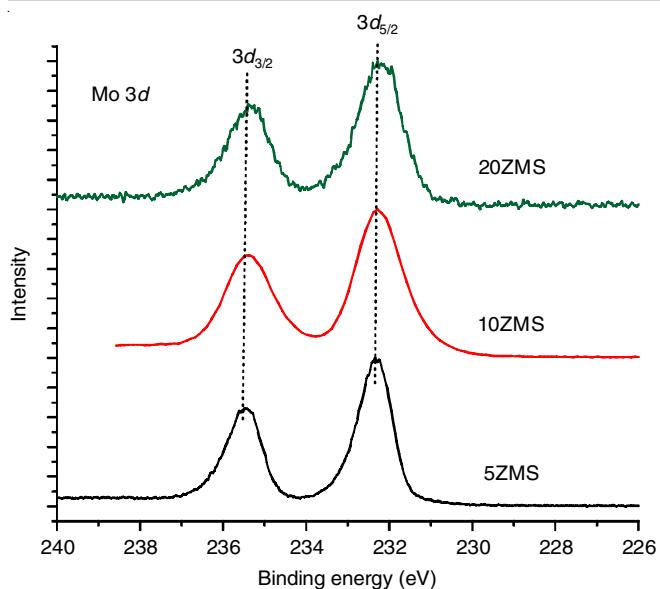| ZrO_2 loading (wt.%)	O $1s$	Si $2p$	Mo $3d_{3/2}$	Mo $3d_{5/2}$	Zr$3d_{3/2}$	Zr$3d_{5/2}$
5 wt.% $ZrO_2/MoO_3/SiO_2$	531.6	103.0	232.36	235.5	182.3	184.5
10 wt.% $ZrO_2/MoO_3/SiO_2$	531.6	103.0	232.29	235.42	182.0	184.46
20 wt.% $ZrO_2/MoO_3/SiO_2$	530.0	102.95	232.21	235.3	181.95	184.4

Fig. 11. Mo 3*d* XPS spectra of ZMS catalysts

O 1*s*: The observed binding energy of O 1*s* in the prepared ZMS samples showed the shifting of peak from 532.5 eV to 530 eV as shown in Fig. 12, which is due to the increase amount of zirconia loading. The additional peak was observed at binding energy 535 eV, which may due to silica lattice oxygen [27].
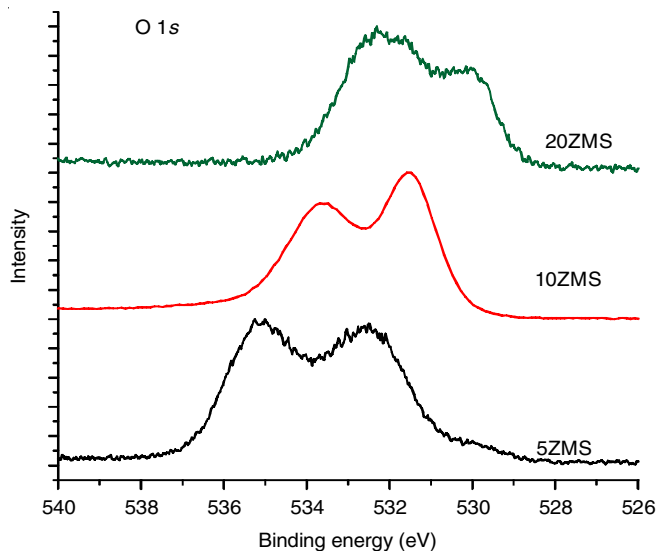
Fig. 12. O 1*s* XPS spectra of ZrO₂/MoO₃/SiO₂ catalysts

Si 2*p*: The Si 2*p* energy region of all the prepared samples indicated the presence of a symmetrical line at 103 eV (Fig. 13), which correspond to O-Si-O and O-Si from SiO₂ phase.

C 1*s*: The C 1*s* binding energies of catalysts was observed at 284.3-285.5 eV (Fig. 14), which correspond to sp^2 and sp^3 carbon.

Catalytic activities: The catalytic activities of synthesized ZMS samples were studied by oxidation of sulphide at different reaction parameters, thioanisole was selected as a model substrate.
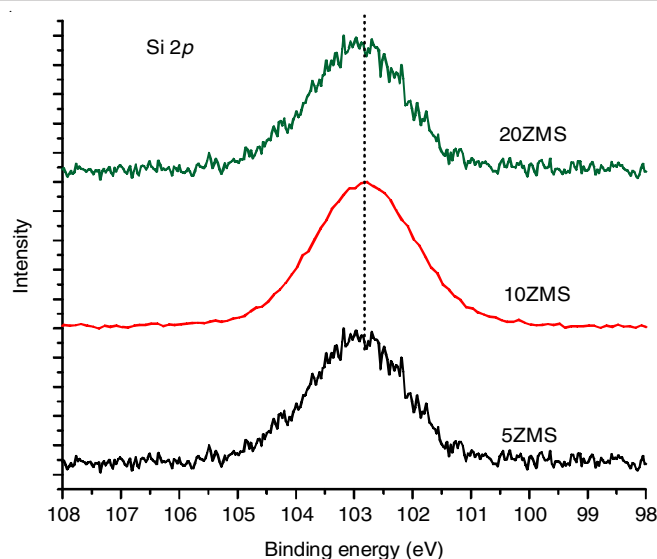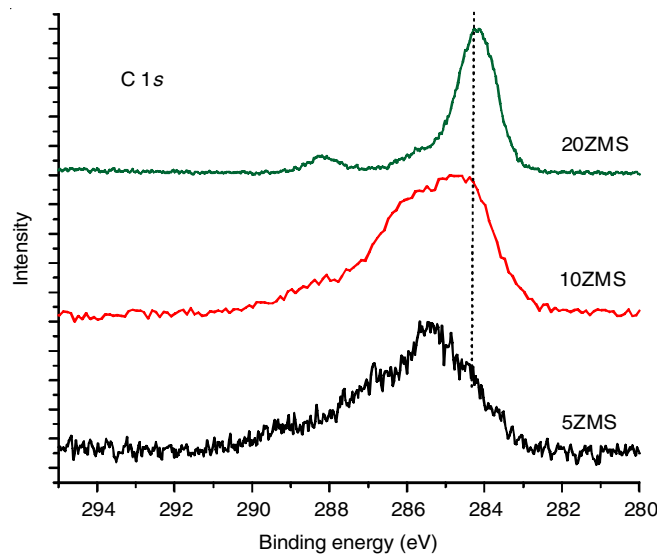

Fig. 13. Si 2*p* XPS spectra of ZMS samples

Fig. 14. C 1*s* XPS spectra of the different composition of Zr on MoO₃/SiO₂ catalysts

Optimization of different catalysts: A series of oxidation reactions of sulfides were carried out over different loading of zirconia *i.e.* 1, 5, 10, 15 and 20 wt. % on MoO₃/SiO₂ catalysts under the optimized condition and the results are shown in Table-4. The reaction was carried out on 20ZMS sample, where the conversion of thioanisole was highest (99.4%), possibly because of the presence of strong acid sites. This is explained by the TPD spectra, which show that 20%ZMS has strong acid sites and no weak acid sites are present. This is due to the increased amount of zirconia on molybdenum, which completely covered the surface of catalyst. The total acidity of 20 ZMS was 0.13 mmol/g, therefore further studies was carried out by using 20%ZMS.

Optimization of catalyst amount: Different amount of ZMS catalyst from 0.02 to 0.30 g were used for the oxidation of sulfides. It was found that the conversion of sulfide increased with the increasing in catalyst amount, that might be due to availability of more active sites at higher catalyst amount.

TABLE-4		
OPTIMIZATION OF DIFFERENT CATALYSTS		
Catalysts	Conversion of thioanisole	Sulfoxides selectivity (%)
1ZMS	98.8	91
5ZMS	95.8	94
10ZMS	87.8	90
15ZMS	95.5	96

Reaction condition: Thioanisole = 1 mmol, H_2O_2 = 2 mmol, solvent = ACN, Retention time = 30 min.

The maximum conversion up to 99.4% of thioanisole was obtained with 0.1 g of 20 wt.% ZMS catalyst (Fig. 15). Further increased the amount of catalyst the conversion remain nearly same but selectivity of methyl phenyl sulfoxide was slightly decreased, which is likely due to further oxidation of sulfoxide into sulfone caused by the excess amount. Therefore, 0.1 g catalyst amount was chosen for further reactions.
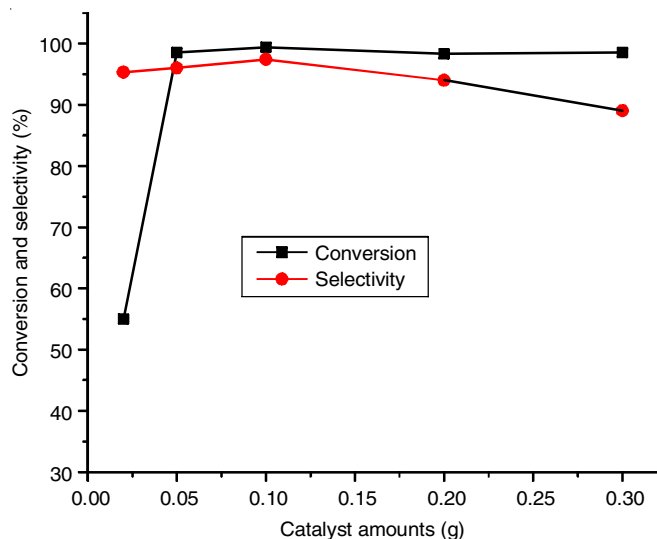

Fig. 15. Effect of catalyst amount (Reaction condition: thioanisole = 1 mmol, H_2O_2 = 2 mmol, solvent = ACN, retention time = 30 min)

Optimization of oxidant amount: The effect of oxidant amount on the oxidation of sulphides to corresponding sulfoxides was studied. The hydrogen peroxide as green oxidant was selected for this reaction under optimized conditions with varying the volume of H_2O_2 from 1, 1.5, 2 and 3 mmol. From Fig. 16, it was observed that as amount of H_2O_2 increased from 1 to 2 mmol, the conversion of sulphide increased (from 40.3% to 99.4%) and 97.3% selectivity of sulfoxide obtained, while further increasing of H_2O_2 showed decrease in selectivity of sulfoxide from 97.3% to 35%. This decrease in selectivity due to increase the amount of oxygen ion in reaction at higher amount of oxidant, which leads to over-oxidation reaction of thioanisole to sulfon therefore, 2 mmol oxidant was selected and used for further oxidation reaction.

Optimization of solvent: Different solvents having different polarity were chosen for this reaction (acetonitrile, toluene methanol and water), the reactions were carried out at room temperature under optimized conditions. The order effect of solvents over the conversion of thioanisole was in range of acetonitrile > toluene > methanol > water > without solvent (Fig. 17).
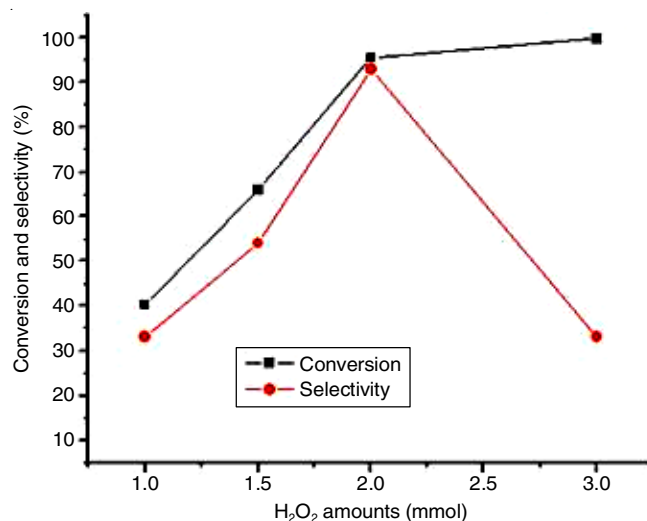

Fig. 16. Effect of oxidant amount (reaction conditions: thioanisole = 1 mmol, catalyst = 0.1 g of 20ZMS, solvent = ACN, retention time = 30 min)
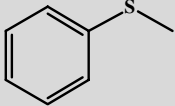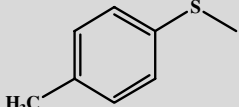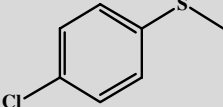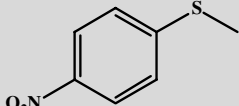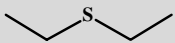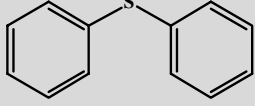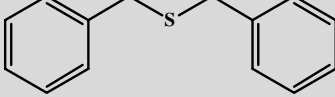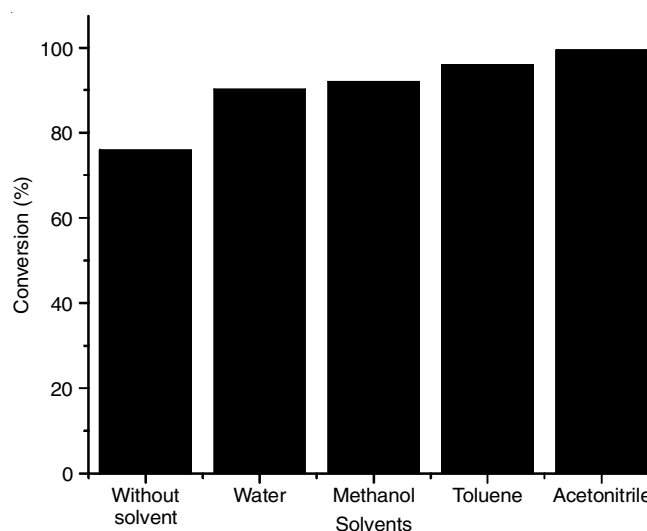

Fig. 17. Effect of solvent on oxidation of sulphide (Reaction condition: thioanisole = 1 mmol, H_2O_2 = 2 mmol, 0.1 g of 20ZMS, retention time = 30 min)

For aprotic solvents, acetonitrile gave good result with 99.4% conversion of thioanisole and 97.39% selectivity of methyl phenyl sulfoxide, the other solvents showed less conversion as compared to acetonitrile, which may be due to low solubility of aqueous hydrogen peroxide in non-polar solvents (water and methanol), while acetonitrile begin polar with dielectric constant was easily dissolved in aqueous H_2O_2 along with thioanisole which makes it easier the adsorption of reaction on the surface of ZMS catalyst and increases in conversion, hence acetonitrile was selected for the further oxidation reaction.

Oxidation of various sulphides: Oxidation of sulfides with 30% H_2O_2 were carried out under suitable reaction conditions at room temperature in presence of 0.1 g 20ZMS catalyst using sulphide:hydrogen peroxide (H_2O_2) volume ratio 1:2 in ACN as solvent. The results (Table-5) showed that ZMS mixed oxide catalysts usable for the oxidation of different sulfides including dialkyl, benzylalkyl and arylalkyl substituted sulphide with H_2O_2 as green oxidant. Among these, thioanisole

TABLE-5
OXIDATION OF DIFFERENT SULFIDES

Entry No.	Sulfide	Time (min)	Conversion (%)	(%) Selectivity of sulfoxide
1		30	99.4	97.39
2		30	99.9	90.0
3		30	99.7	92.5
4		30	95.6	85.3
5		120	89.1	100.0
6		45	82.0	87.0
7		45	92.8	90.1

gave higher conversion (99.4%) than biphenyl sulphide (Table-5, entries 6) meanwhile, it was observed the significant effects of electronic and steric factors of substrates on conversion and selectivity [28]. In general, sulphides with electron-rich side group *i.e.* high electron density on sulphur atom in sulphide such as methyl-*p*-tolyl sulphide was oxidized at higher conversion than sulphide with electron-deficient group such as 4-nitro-thioanisole (Table-5, enter 4).

Recycling and reuse of catalyst: In order to estimate the stability of prepared ZMS catalyst after completion of reaction, the catalyst was washed, dried, then calcined at 500 °C and used for oxidation reaction with fresh reaction mixture. The ZMS catalyst was still active and reusable without any loss of activity toward oxidation reaction for three cycles (Fig. 18).

Plausible mechanism of oxidation of sulphide: The plausible mechanism for the oxidation of sulfides over ZMS catalyst is presented in Fig. 19. Hydrogen peroxide reacted with the active sites of ZMS catalyst to generate peroxy species, which in turn reacted with sulphide to form an intermediate; finally then this intermediates combined to form sulfoxide with water as byproduct. This might be due to the strong acidity of $ZrO_2/MoO_3/SiO_2$ catalyst.

Conclusion

By using sol gel method, $ZrO_2/MoO_3/SiO_2$ catalysts with various loading were synthesized and characterized by FT-IR, Raman, XRD, SEM, EDX, TEM and XPS techniques. In most of the synthesized catalyst, effective tetragonal phase geometry was found to be more operative for the catalytic study. The
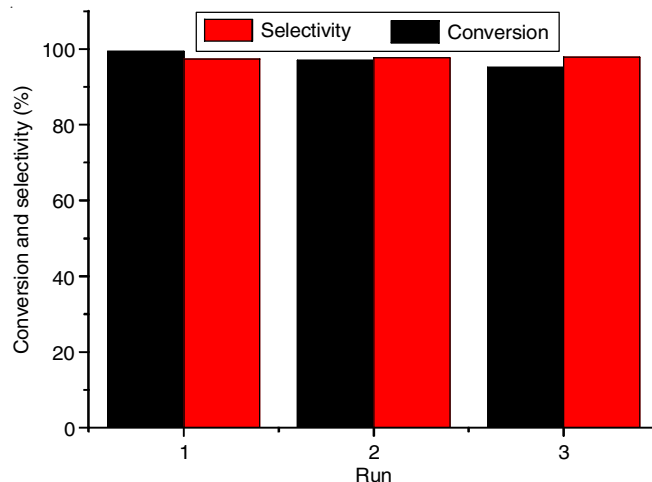

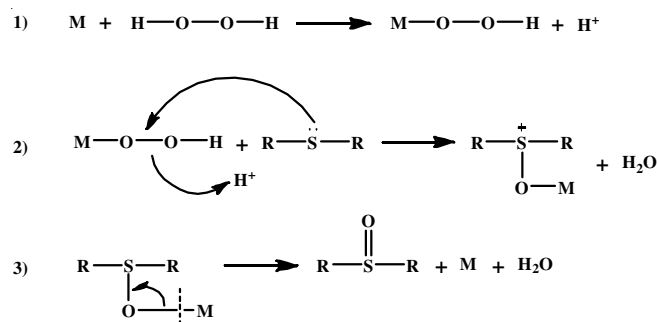
Fig. 18. Recycling and reuse of catalyst

Fig. 19. Mechanism of oxidation reaction of sulphide

oxidation of sulfides to sulfoxides was carried out using 30% H_2O_2 as green oxidant which results in high conversion, 99.4% towards sulfoxides. ZMS catalyst was found non-corrosive, inexpensive, environmental benign and can be reused by simple filtration method without significant loss in the catalytic performance and gave excellent conversion of reactant and selectivity of product.

CONFLICT OF INTEREST

The authors declare that there is no conflict of interests regarding the publication of this article.

REFERENCES

1. L. Liu and A. Corma, *Chem. Rev.*, **118**, 4981 (2018);
   https://doi.org/10.1021/acs.chemrev.7b00776
2. Q. Jia, S. Ghoshal, J. Li, W. Liang, G. Meng, H. Che, S. Zhang, Z.-F. Ma and S. Mukerjee, *J. Am. Chem. Soc.*, **139**, 7893 (2017);
   https://doi.org/10.1021/jacs.7b02378
3. A. Guldhe, P. Singh, F.A. Ansari, B. Singh and F. Bu, *Fuel*, **187**, 180 (2017);
   https://doi.org/10.1016/j.fuel.2016.09.053
4. S.B. Rathod, M.K. Lande, B.R. Arbad and A.B. Gambhire, *Arab. J. Chem.*, **7**, 253 (2014);
   https://doi.org/10.1016/j.arabjc.2010.10.027
5. S. Wang, C. Li, Z. Xiao, T. Chen and G. Wang, *J. Mol. Catal. Chem.*, **420**, 26 (2016);
   https://doi.org/10.1016/j.molcata.2016.04.002
6. D. Sun, S. Chiba, Y. Yamada and S. Sato, *Catal. Commun.*, **92**, 105 (2017);
   https://doi.org/10.1016/j.catcom.2017.01.010
7. M.R. Dumont, E.H.M. Nunes and W.L. Vasconcelos, *Ceram. Int.*, **42**, 9488 (2016);
   https://doi.org/10.1016/j.ceramint.2016.03.021
8. E.B. Silveira, R.C. Rabelo-Neto and F.B. Noronha, *Catal. Today*, **289**, 289 (2016);
   https://doi.org/10.1016/j.cattod.2016.08.024
9. H.J. Lee, D.-C. Kang, S.H. Pyen, M. Shin, Y.-W. Suh, H. Han and C.-H. Shin, *General*, **531**, 13 (2017);
   https://doi.org/10.1016/j.apcata.2016.11.032
10. M. Hino and K. Arata, *J. Chem. Soc. Chem. Commun.*, 851 (1980);
    https://doi.org/10.1039/C39800000851
11. L.I. Bikmetova, M.D. Smolikov, E.V. Zatolokina, K.V. Kazantsev, V.Yu. Tregubenko and A.S. Belyi, *Procedia Eng.*, **152**, 87 (2016);
    https://doi.org/10.1016/j.proeng.2016.07.634
12. S.S. Kahandal, A.S. Burange, S.R. Kale, P. Prinsen, R. Luque and R.V. Jayaram, *Catal. Commun.*, **97**, 138 (2017);
    https://doi.org/10.1016/j.catcom.2017.03.017
13. A. Rachmat, W. Trisunaryanti, Sutarno and K. Wijaya, *Mater. Renew. Sustain. Energy*, **6**, 13 (2017);
    https://doi.org/10.1007/s40243-017-0097-1
14. A.D. Vaizogullar, A. Balci and M. Ugurlu, *Indian J. Chem.*, **54A**, 1434 (2015).
15. A.K. Arora, V.S. Jaswal and R. Bala, *Asian J. Res. Chem.*, **11**, 893 (2018);
    https://doi.org/10.5958/0974-4150.2018.00155.4
16. K. Ni, L.-G. Meng, H. Ruan and L. Wang, *Chem. Commun.*, **55**, 8438 (2019);
    https://doi.org/10.1039/C9CC04090K.
17. W. Wei, H. Cui, D. Yang, H. Yue, C. He, Y. Zhang and H. Wang, *Green Chem.*, **19**, 5608 (2017);
    https://doi.org/10.1039/C7GC02330H
18. K.-J. Liu, J.-H. Deng, J. Yang and S.-F. Gong, Y.-W. Lin, J.-Y. He, Z. Cao and W.-M. He, *Green Chem.*, **22**, 433 (2019);
    https://doi.org/10.1039/C9GC03713F
19. B. Yu, A.-H. Liu, L.-N. He, B. Li, Z.-F. Diao and Y.-N. Li, *Green Chem.*, **14**, 957 (2012);
    https://doi.org/10.1039/c2gc00027j
20. R.A. Nyquist, C.L. Putzig and M.A. Leugers, Handbook of Infrared and Raman Spectra of Inorganic Compounds and Organic Salts, vol. 3, Academic Press: New York (1997).
21. G.B. Rayner Jr., Ph.D. Thesis, Department of Physics, North Carolina State University, Raleigh, USA (2002).
22. M.M. Mohamed, T.M. Salama and T. Yamaguchi, *Colloids Surf. A*, **207**, 25 (2002);
    https://doi.org/10.1016/S0927-7757(02)00002-X
23. N.S. Hassan, A.A. Jalil, S. Triwahyono, C.N.C. Hitam, A.F.A. Rahman, N.F. Khusnun, C.R. Mamat, M. Asmadi, M. Mohamed, M.W. Ali and D. Prasetyoko, *J. Taiwan Inst. Chem. Eng.*, **82**, 322 (2018);
    https://doi.org/10.1016/j.jtice.2017.10.038
24. J. Adamiak, W. Tomaszewski and W. Skupiñski, *Catal. Commun.*, **29**, 92 (2012);
    https://doi.org/10.1016/j.catcom.2012.09.026
25. H. Bala, W. Fu, J. Zhao, X. Ding, Y. Jiang, K. Yu and Z. Wang, *Colloids Surf. A Physicochem. Eng. Asp.*, **252**, 129 (2005);
    https://doi.org/10.1016/j.colsurfa.2004.10.064
26. Y.V. Plyuto, I.V. Babich, I.V. Plyuto, A.D. Van Langeveld and J.A. Moulijn, *Appl. Surf. Sci.*, **119**, 11 (1997);
    https://doi.org/10.1016/S0169-4332(97)00185-2
27. I. Sulym, D. Sternik, L. Oleksenko, L. Lutsenko, M. Borysenko and A. Derylo-Marczewska, *Surf. Interfaces*, **5**, 8 (2016);
    https://doi.org/10.1016/j.surfin.2016.08.001
28. C. Wu, X. Zhao, Y. Ren, Y. Yue, W. Hua, Y. Cao, Y. Tang and Z. Gao, *J. Mol. Catal. Chem.*, **229**, 233 (2005);
    https://doi.org/10.1016/j.molcata.2004.11.029